JOURNAL OF PROPULSION AND POWER
Vol. 16, No. 5, September–October 2000

Ion-Energy Diagnostics in the Plasma Exhaust Plume of a Hall Thruster

Lyon B. King* and Alec D. Gallimore†
University of Michigan, Ann Arbor, Michigan 48105

Of primary concern with the integration of Hall thrusters on conventional satellite designs is the possible damaging effect of high-energy exhaust ions impinging upon spacecraft surfaces. This paper reports on measurements of plasma ion-energy distributions within the plume of an SPT-100 Hall thruster using a custom-designed molecular-beam mass spectrometer. With this instrument ion energy was measured over a complete 360-deg circumference about the thruster at a radius of 0.5 m from the exit plane and over a total inclusive arc of 260 deg at 1.0-m radius. These data uncovered the existence of high-energy ions departing the thruster at angles exceeding 90 deg from the thrust vector and continuing well into the backflow region of the plume. Through an analysis of the energy structure, the evidence of charge-exchange collisions occurring between plume ions and background neutrals was documented; such collisions produced anomalous distributions of ions having voltages greater than that applied to the thruster discharge.

Nomenclature

A_c	= area of collector, m^2
d	= analyzer plate separation, m
E_i	= ion energy, J or eV
e	= elementary charge, C
$f(u_i)$	= ion velocity distribution, s/m
$f(V_i)$	= ion voltage distribution, s/m
G_{CEM}	= gain of electron multiplier
K_{45}	= spectrometer constant
k	= Boltzmann constant, J/K
L	= analyzer interslit distance, m
m_i	= mass of ion, kg
n_i	= ion density, m^{-3}
q	= ion integer charge state
r	= radial distance from thruster, m
u_i	= ion velocity, m/s
V_b	= main distribution voltage, V
V_i	= ion voltage, V
V_m	= most-probable voltage, V
V_p	= repelling plate voltage, V
w	= analyzer slit width, m
x	= spatial coordinate, m
y	= spatial coordinate, m
θ	= angle, deg
τ_i	= distribution half-width at e^{-1} point, V

I. Introduction

OF primary concern with the use of Hall thrusters on geostationary communications satellites is the possible damaging effect of the highly energetic plasma exhaust plume on spacecraft surfaces. Specific issues include the erosion of solar array material because of incident high-energy propellant ions, coating, and contamination of solar arrays and other surfaces caused by efflux of thruster self-erosion material, heating of sensitive spacecraft components, and uneven spacecraft charging caused by impinging propellant ions. To fully quantify and understand these phenomena, extensive characterization of the plasma plume has been performed over the past few years.

The initial effort toward characterizing the Hall-thruster plume was undertaken by a joint industry team composed of Russian and U.S. researchers.[1] This test used a set of sample slides representative of spacecraft surfaces placed in the plume flow to model erosion and contamination in addition to the use of a Faraday probe to measure ion current density and a gridded retarding potential analyzer (RPA) to measure the ion-energy distribution. Because of the rapid decay in ion density with increasing distance from the thruster centerline (thrust vector), these diagnostics were limited to points lying within 60 deg of the thrust vector. Within this volume, however, the RPA data demonstrated some intriguing trends. Although the thruster discharge voltage was set to 300 V, the ion-energy distribution curve showed a significant tail representing ions accelerated through potentials as great as 350–450 V (Ref. 1). Possible reasons for the existence of this anomalous high-energy population were not addressed. More plume characterization testing followed: Myers and Manzella performed additional measurements using an RPA, but the data were collected at very few spatial locations within the plume and again were confined to points within 60 deg of the axis.[2] These data, as well, suggested the existence of ions with voltages greater than that supplied by the applied discharge. The region of the plume with the greatest interest for spacecraft designers was the far off-axis region (angles greater than 60 deg from centerline) because of the probable location of spacecraft surfaces. The ion current density in this region (out to 100 deg) was probed by Manzella and Sankovic[3]; however, prior to the study reported here, no ion-energy diagnostics have been performed out to such large angles.

Continued studies of plume-induced erosion and contamination were performed using more extensive test matrices comprising a wide array of representative spacecraft materials exposed to a large volume of the plasma plume, including the far off-axis region.[4,5] For the most part these studies were addressed not at deepening the knowledge of the plasma properties within the plume; instead they documented the erosion/contamination problem from a top-level perspective by simply measuring the net effects of the plume on representative spacecraft materials. For near-term applications of the SPT-100, these top-level studies provided sufficient databases to enable integration of the Hall thruster with western satellites. However, to prevent the need for further extensive sample testing to accommodate new spacecraft materials or design configurations in the future, it was apparent that a more thorough understanding of the underlying physics and properties of the plasma plume was required.

Received 28 November 1998; revision received 28 July 1999; accepted for publication 16 September 1999.

*Graduate Researcher, Plasmadynamics and Electric Propulsion Laboratory, Department of Aerospace Engineering; currently Research Associate, National Institute of Standards and Technology, Time and Frequency Division 847, 325 Broadway, Boulder, CO 80303; lyon.king@boulder.nist.gov. Member AIAA.

†Associate Professor, Plasmadynamics and Electric Propulsion Laboratory, Department of Aerospace Engineering, 1919 Green Road, Room B107; alec.gallimore@umich.edu. Associate Fellow AIAA.

This paper represents one part of a comprehensive study performed at the University of Michigan to characterize the plasma properties within the Hall-thruster plume over a large volume in space including the far off-axis regions as well as the backflow area directly behind the thruster.[6–10] The purpose of this paper is to present measurements of the ion energy acquired through the use of a custom-designed molecular beam mass spectrometer (MBMS) for Hall-thruster research.

II. Description of Apparatus

The MBMS system used a set of orifice skimmers to admit a beam of plume ions from the main vacuum chamber into an array of differentially pumped subchambers. The geometrical design of the MBMS instrument used in this investigation was similar to that of Pollard.[11] The subchambers were maintained at high vacuum to minimize and effectively eliminate collisions involving ions within the beam. A sampling skimmer orifice was mounted on the upstream end of the MBMS; this orifice skimmed off a small diameter ion beam into the first subchamber. This beam was then collimated by a second orifice at the downstream end of the first subchamber. The collimated beam then passed through the entrance slit of a 45-deg electrostatic energy analyzer. This analyzer employed a constant electric field such that only ions with a preselected ratio of energy per charge had a trajectory that permits them to traverse the exit slit and impinge upon a detector. The overall layout of the instrument is shown in Fig. 1. Ion mass detection was possible through a time-of-flight method using an electrostatic beam gate immediately downstream of the sampling skimmer; the mass diagnostics are the subject of a related paper.[6] This paper will focus on the global (species independent) ion-energy distribution, and hence, the beam gate was not used in this study.

The 45-deg electrostatic energy analyzer is a flexible, robust method for particle energy filtering that has been used widely in beam physics research.[12–14] A schematic of the system used in the MBMS is shown in Fig. 2 with coordinate system and relevant dimensions defined. The ion beam is admitted through the entrance slit of the analyzer and immediately enters a region of constant electric field of magnitude V_p/d oriented at an angle θ to the direction of travel. The ions thus experience a constant acceleration in the negative y direction such that the spatial equation of their trajectory is

$$y = x - \frac{q_i e V_p}{2 d m_i} \frac{x^2}{u_i^2 \sin^2 \theta} \tag{1}$$

Because $\theta = 45$ deg and $u_i^2 = 2E_i/m_i$, Eq. (1) becomes

$$y = x - (1/2d)[V_p/(E_i/q_i e)]x^2 \tag{2}$$

For an ion to pass through the analyzer and escape through the exit slit to the detector, it must intersect the point $y = 0, x = L$; this pass constraint is defined as the spectrometer constant K_{45} and is given by

$$K_{45} \equiv [V_p/(E_i/q_i e)] = 2d/L \tag{3}$$

The analyzer thus performs the function of an energy-per-charge filter $E_i/q_i e$. Because the beam ions within the Hall-thruster plume experienced a discharge acceleration according to $q_i e V_i = \frac{1}{2} m_i u_i^2$, the value of energy per charge for an ion is equivalent to the acceleration voltage V_i seen by the ion in the discharge acceleration chamber. For a given value of repelling plate voltage, only ions with

$$V_i = \frac{\frac{1}{2} m_i u_i^2}{q_i e} = \frac{V_p}{K_{45}} \tag{4}$$

will reach the collector and be recorded as ion current. The current detector employed by the MBMS was a ceramic channel electron multiplier (CEM). The CEM had an adjustable gain ranging from 10^6 to 10^8, with an extremely low output dark current of 1×10^{-14} A at low gain and 1×10^{-12} A at high gain.

For a single species flow the 45-deg electrostatic analyzer technique produces an ion current vs repelling voltage trace, which is directly proportional to the ion-energy distribution function, analogous to the RPA technique. However, unlike the RPA technique, the 45-deg analyzer requires no numerical differentiation of raw data to obtain the distribution, and the resultant curves are therefore much more precise and smooth. Unfortunately, like the RPA, the existence of multiple ion species in the beam complicates interpretation of the data, which can be demonstrated by analyzing the output of the CEM. Because the CEM produced a current proportional to the number of ions incident on the collector, the current output can be written as

$$I_i = G_{\mathrm{CEM}} A_c n_i \langle u_i \rangle \tag{5}$$

The current output of the CEM is not dependent upon the charge state q_i of the incoming ions. Instead, the CEM is sensitive only

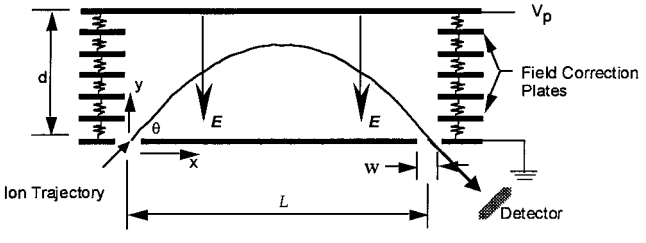

Fig. 2 Schematic of 45-deg electrostatic ion-energy analyzer. A constant electric field is formed by applying repelling voltage to the top plate with the bottom plate grounded. Field correction plates are biased with a voltage divider to force boundary conditions at midplanes, preventing field distortion caused by surrounding ground potential.

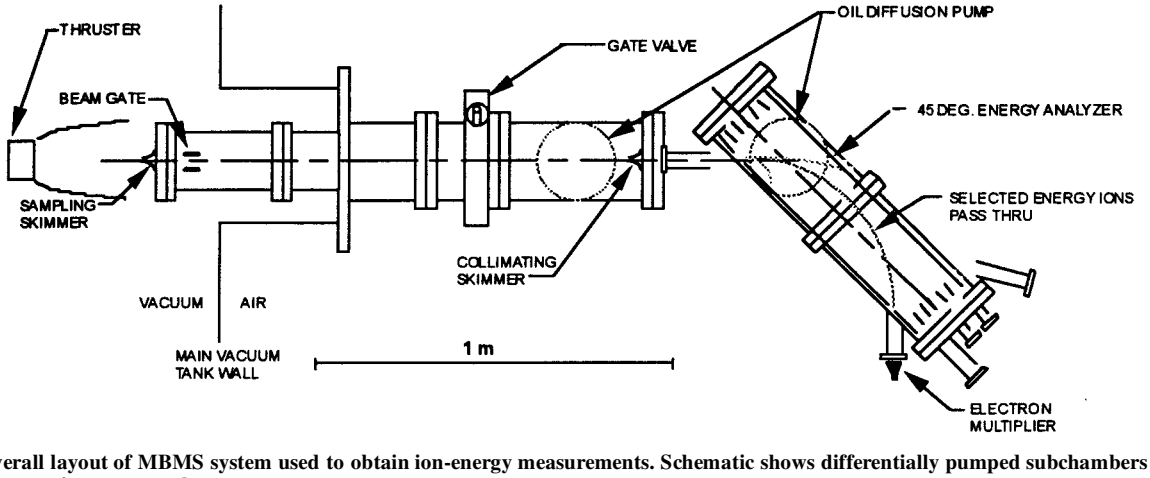

Fig. 1 Overall layout of MBMS system used to obtain ion-energy measurements. Schematic shows differentially pumped subchambers as well as 45-deg electrostatic energy analyzer.

Table 1 Physical characteristics and resolving power of 45-deg electrostatic energy analyzer

Parameter	Value
d	160 mm
L	584 mm
w	3 mm
K_{45}	0.549
$\Delta V_i / V_i$	0.004

to the number flux of ions, and, thus, I_i is not proportional to q_i. According to Eq. (4), only ions with a discrete voltage V_i will be detected by the CEM such that

$$I_i(V_i) = G_{\mathrm{CEM}} A_c n_i(V_i) \sqrt{2 q_i e V_i / m_i} \tag{6}$$

where $n_i(V_i)$ is the number density of ions with voltage V_i, which is the ion voltage distribution function $n_i(V_i) = f(V_i) = f(E_i/q_i e)$. Realizing this fact, it is apparent from Eq. (6) that the ion current vs voltage is not directly proportional to the ion-energy distribution function as is widely accepted with these devices. Rather, in a multicomponent ion beam the 45-deg energy analyzer yields data that are related to the voltage distribution function according to

$$f(V_i) \propto \frac{I_i(V_i)}{\sqrt{q_i e V_i}} \tag{7}$$

The 45-deg electrostatic energy analyzer was constructed of 1.5-mm-thick aluminum plates. To eliminate field distortion within the analyzer caused by the surrounding ground potential of the vacuum chamber walls and to ensure a homogeneous electric field, a set of seven centrally slotted field-correction plates were mounted intermediate to the repelling plate and the entrance ground plate. These correction plates were biased using a resistor string voltage divider to force the electric equipotentials at the midplanes and minimize field leakage. The entire plate system was supported on a frame constructed of $\frac{3}{16}$-in.-diam nylon threaded rods to ensure electrical isolation of each plate. The resolving power of the analyzer is dictated by geometric parameters and is given by

$$\Delta V_i / V_i = w \sin\theta / L \tag{8}$$

The pertinent parameters of the 45-deg electrostatic energy analyzer used in the MBMS for this research are presented in Table 1.

III. Experimental Setup

The experiments reported in this paper were performed in a 6-m-diam × 9-m-long stainless-steel vacuum chamber at the University of Michigan. The facility is supported by six 81-cm-diam oil diffusion pumps (with water-cooled coldtraps), backed by two blowers and four mechanical pumps. These pumps give the facility an overall air-pumping speed of approximately 150,000 L/s at 1 mPa. Chamber pressure was measured with hot-cathode ionization gauges that were corrected for xenon located on vacuum ports on either side of the chamber. Background chamber pressure was maintained at less than 4 mPa when the Hall thruster was operating on approximately 5 mg/s of xenon.

The thruster used in this research was a flight model SPT-100 manufactured by the Fakel Design Bureau. The SPT-100 was operated at nominal conditions of 300 V at 4.5-A discharge as controlled through a power-processing unit manufactured by Space Systems/Loral. The propellant flow rate was 5 mg/s with 7% of the total flow diverted through the hollow cathode. The SPT-100 was mounted to a rotary table such that the rotation axis coincided with the center of the exit plane of the thruster. Therefore, by rotating the thruster relative to the fixed MBMS skimmer inlet the plasma plume could be sampled as a function of angular position at a fixed radial distance r from the exit plane. This setup is illustrated schematically in Fig. 3. Facility surfaces subject to plume impingement were coated

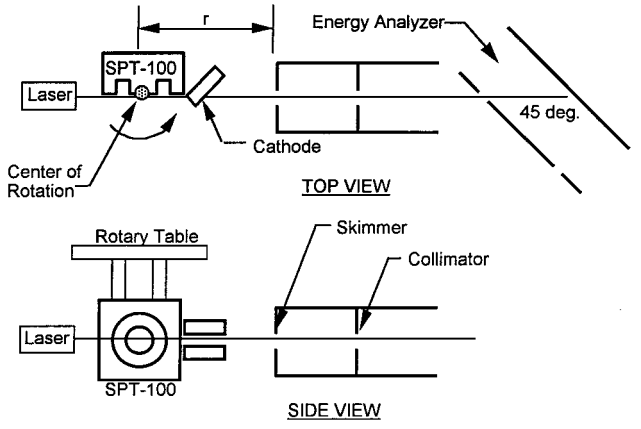

Fig. 3 Experimental setup diagram showing rotary thruster mount and laser alignment of beam line.

with flexible graphite foil. The centerline (thrust axis) of the thruster was denoted as 0 deg, with positive theta values representing points in the cathode half-plane of rotation (the angular position shown in Fig. 3 represents $\theta = +90$ deg). The angular alignment of the thruster and MBMS was achieved by using a laboratory laser to establish the MBMS beam line. The laser beam line was used to verify the angular orientation of the 45-deg electrostatic analyzer to within 0.5 deg; similarly, the thruster was rotated such that the laser beam line was precisely aligned with the center of the exit plane of the thruster, as shown in Fig. 3, establishing the 90-deg position of the SPT-100 to better than 0.5 deg. Because the relative uncertainty in angular position of the rotary table was 0.1 deg, the uncertainty in position for all data points is ± 0.5 deg because of initial alignment uncertainty. By relocating the rotary table mount between tests, data were obtained as a function of angular position for radial distances from the thruster of $r = 0.5$ and 1.0 m.

The 45-deg analyzer repelling voltage was supplied by slowly varying the output of a high-precision sourcemeter. The sourcemeter provided regulated voltage with better than 0.012% accuracy over a range of 0 to 1100 V. The CEM current was measured with a sensitive picoammeter and recorded as a function of 45-deg analyzer pass voltage. By using the picoammeter, the high-gain CEM, and long sampling times true ion currents as low as 5×10^{-19} A could be accurately measured.

IV. Ion Voltage Measurements

The ion current incident on the CEM was recorded as a function of ion voltage by varying the repelling potential on the 45-deg energy analyzer. In this fashion curves were obtained at a radial distance of 0.5 m from the thruster exit plane as a function of angular position about the thrust axis in 10-deg intervals. The high gain achieved with the picoammeter and CEM enabled data to be obtained in a complete 360-deg envelope about the SPT-100. Peak measured ion current values fell as low as 1×10^{-18} A for points directly behind the thruster. These sweeps are summarized in Figs. 4 and 5. The entire data sets can be found in Ref. 15. The abscissa of the ion current curves have been corrected for the energy imparted to the ions as they fell from ambient plasma potential through the skimmer inlet to ground potential; the magnitude of the required correction was obtained using a Langmuir probe immediately upstream of the sampling skimmer to measure the local plasma potential.[16]

The ion-energy distribution function was evaluated at a radial distance of 1.0 m from the thruster exit plane by repositioning the thruster/rotary table mount relative to the MBMS inlet skimmer. At this distance curves were obtained as a function of angular position about the SPT-100 thrust axis. Because of the much lower ion densities at 1.0 m as compared with those at 0.5 m, data could not be obtained in a complete 360-deg arc about the thruster. The region behind the thruster at positive angles greater than 110 deg and negative angles of magnitude greater than −150 deg represented

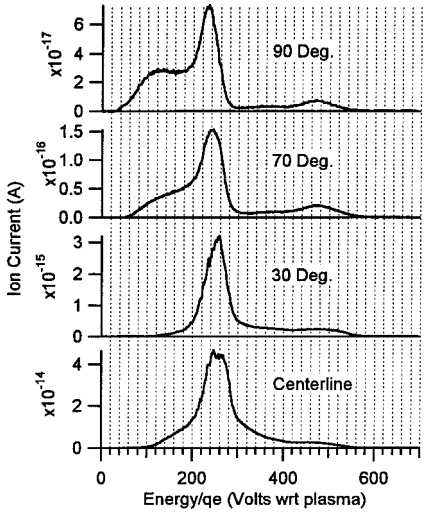

Fig. 4 Ion energy from centerline to 90 deg off axis at 0.5-m radius from thruster exit plane.

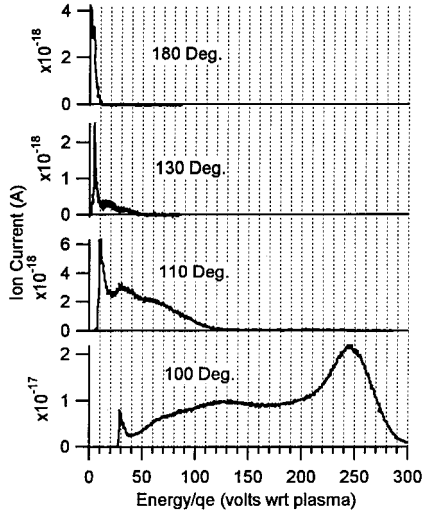

Fig. 5 Ion energy in backflow region at 0.5-m radius from thruster exit plane.

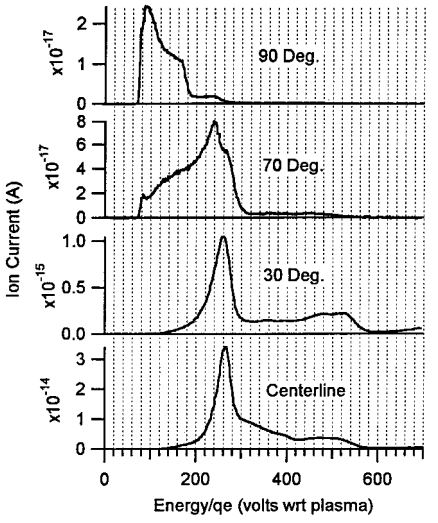

Fig. 6 Ion-energy distribution from centerline to 90 deg at 1.0-m radius from thruster exit plane.

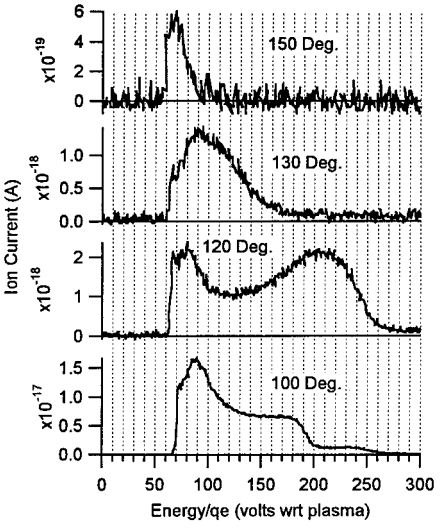

Fig. 7 Ion-energy distribution in the backflow region at 1.0-m radius from thruster exit plane.

ion currents less than 5×10^{-19} A; because of the low currents, this region could not be evaluated. The resulting data are shown in Figs. 6 and 7. These curves have been corrected for the parasitic energy addition imposed to the ions as they fell from local plasma potential through the inlet skimmer to ground potential.

The ion current traces obtained at 1.0-m radius for the points near 10 deg were strikingly dissimilar from the overall trends exhibited as a function of angular position. To more fully interrogate this region of the plume, data were obtained with much finer angular resolution for points within 20 deg of the axis. The general behavior of the points near 10 deg off axis are represented in Fig. 8.

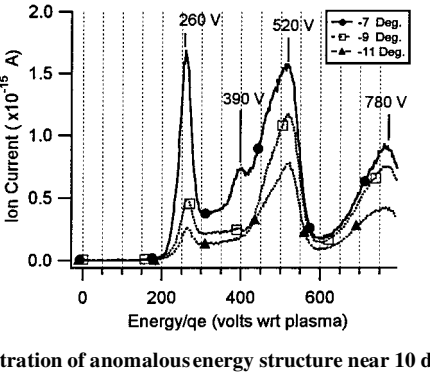

Fig. 8 Illustration of anomalous energy structure near 10 deg off axis at 1.0 m from thruster. Note the existence of discrete distributions of ions having voltages greater than the 300 V applied to the thruster discharge.

V. Discussion of Ion Voltage Distributions

The relation linking the $I(V)$ curve to the ion voltage distribution function was already derived: as evidenced by Eq. (7), calculation of the voltage distribution in a multispecies flow requires knowledge of the ionization-state-dependent current as a function of voltage. Specifically,

$$f(V) \propto \frac{1}{\sqrt{V}}\left[\frac{I(V,q_1)}{\sqrt{q_1}} + \frac{I(V,q_2)}{\sqrt{q_2}} + \cdots\right] \tag{9}$$

where $I(V, q_n)$ denotes the current caused by ions with voltage V and charge q_n. Because ion velocity increases with q, a population of high-q ions will produce a larger current than an equal number of low-q ions: The inclusion of $q^{-1/2}$ in Eq. (9) is therefore required to account for the disproportional contribution of high-q ions to the total ion current. The data reported in this paper reflect the total current caused by all ion charge states as a function of ion voltage; therefore, they cannot be directly manipulated to yield $f(V)$. If the flow under consideration was composed almost entirely of one species of ion ($q = 1$), then it would be possible to obtain a good approximation of $f(V)$ by neglecting the contribution caused by

the higher charge states. This approximation has previously been applied to the RPA technique allowing valuable estimations of ion density and velocity to be made in the region of the plume near thruster centerline.[7,15]

Although the $I(V)$ curve is not directly proportional to $f(V)$ for reasons just discussed, it should be kept in mind that these two functions are very closely related. For example, if a portion of the $I(V)$ curve was known to result entirely from ions with $q = 2$, attenuation of this portion of the curve by a factor of 0.707 would yield the value of $f(V)$. Allowing for the existence of ions with charge states up to $q = 4$ in the flow ensures that the value of $I(V)$ is never more than a factor of two larger than $f(V)$. Therefore, although it may be inappropriate to substitute $I(V)$ for $f(V)$ in detailed calculations, when discussing the overall shape and data trends it is reasonable to speak of the two functions interchangeably.

A. Ion Distribution Width

Because the $I(V)$ traces obtained with the 45-deg analyzer very closely approximate the ion voltage (energy) distribution function, it is perhaps instructive to describe their shape in terms of an ion temperature. However, the driving mechanism defining the shape of the $I(V)$ curves is believed to be an overlap between the ionization region and acceleration region within the SPT-100 discharge chamber: ions are created throughout a region in space over which the potential varies greatly, thus the spread in the $I(V)$ curve reflects the fact that ions are born in regions of different potential and therefore experience different acceleration voltages. This spread is likely not equal to the equilibrium thermal variation in ion energy. To provide a figure of merit for discussing the width in the measured distributions, the parameter τ_i will be defined as the half-width of the $I(V)$ distribution at the point in the curve where $I(V)$ is equal to e^{-1} times $I(V_m)$, where V_m represents the most probable voltage such that $I(V_m)$ is a maximum. Because the distribution functions were not symmetric about V_m, the parameter τ_i can take on either of two values corresponding to the e^{-1} point with voltage larger or smaller than V_m. For discussion purposes τ_i was defined at the $e^{-1} f(V_m)$ point such that $V > V_m$ (to the right of the peak).

The 0.5-m $I(V)$ data sets exhibited interesting general trends in width. The interpretation of τ_i was somewhat confused by the existence of multiple peaks for the angular positions centered around 90 and -90 deg; for these traces it was unclear which peak defined the main distribution.[15] However, for many of the angular positions the distribution was characterized by a single dominant peak, which was used to calculate τ_i. Figure 9 shows a plot of τ_i as a function of angular position for arcs lying at 0.5 and 1.0 m from the SPT-100 exit plane. Values of τ_i were not calculated for points in which the choice of dominant distribution peak was unclear.

Variation in the distribution width for points lying along the 1.0-m radius is included in the plot of Fig. 9. However, the anomalous distributions found between 5 and 20 deg of thrust axis prevented calculation of a meaningful τ_i for these points: the distribution in this regime consisted of multiple current peaks with comparable magnitudes such that the choice of a dominant distribution was not clear.[15] This fact created gaps in the τ_i vs θ plot and hindered the identification of trends.

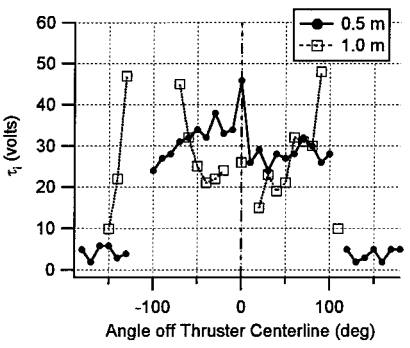

Fig. 9 Variation of distribution half-width τ_i as a function of angular position at 0.5- and 1.0-m radius from the SPT-100 exit plane. Uncertainty in $\tau_i < 1$ V.

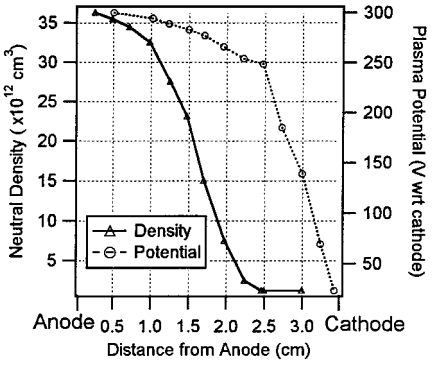

Fig. 10 Neutral propellant density and local plasma potential within the Hall-thruster acceleration layer as modeled by Baranov.[17]

The calculated values for τ_i shown in Fig. 9 demonstrate excellent agreement with the currently accepted structure of the ionization and acceleration regions within the SPT-100 discharge chamber. Baranov et al.[17] have recently developed a comprehensive model of the acceleration layer formation within the Hall thruster. This model was used to predict plasma parameters such as electron temperature, plasma density, collision frequencies, and electric field within the acceleration region of a Hall thruster very similar to the SPT-100. The neutral atom density and plasma potential predictions resulting from this model are reproduced as Fig. 10.

In this model, as in actual Hall-thruster operation, neutral propellant is injected through the anode. This propellant is then ionized by electron collisions as the neutral atoms travel towards the cathode. The decay in neutral atom density with distance from the anode therefore corresponds to the disappearance of neutrals caused by ionization. As can be seen from the model, most of the propellant is ionized within a region extending 2.5 cm from the anode. Within this ionization region the local plasma potential varies from 300 to 250 V, thus the ions that are born within this region will have a voltage spread of approximately 50 V upon exiting the discharge chamber. This agrees with the measured values of τ_i (half-width) of approximately 20–40 V for the main discharge ion beam within 90 deg of thrust axis shown in Fig. 9. Furthermore, many of the ions formed within the first 2.5 cm of the anode will likely suffer a neutralizing collision with the discharge chamber wall downstream, followed by a second (or even third) ionizing electron collision; these ions will increase the spread in the exhaust voltage distribution beyond that induced by the 2.5-cm ionization zone.

The population of ions behind the thruster (at angles greater than about 100 deg) possess considerably narrower distributions than the main beam ions as expected. However, this backflow plasma still has a value of τ_i ranging between 2 and 5 V. Although no investigations of the Hall-thruster backflow regions were performed prior to this study, it was widely accepted that this region most likely consisted of macroscopically stagnant plasma arising from charge-exchange collisions between plume ions and background facility gas caused by vacuum chamber pumping limitations, thus the distribution would have a width on the order of the local ambient neutral temperature (300 K, or about 0.03 eV). However, it is very unlikely that the high temperature implied by the width of the measured voltage distribution in the backflow (of roughly 50,000 K) represents a true thermal spread within a macroscopically stagnant plasma as would be expected to exist behind the thruster. The physical mechanism producing such a wide energy spread in the backflow ions is unknown as of this writing. Further characterization of the backflow region is necessary.

B. Most-Probable Voltage

Another measure of the ion-energy structure, the most-probable ion voltage, was compiled as a function of angular position. This voltage was easily defined and identifiable on all plots as the voltage (energy/q) corresponding to the maximum in the $I(V)$ vs V curve. This quantity is plotted for both 0.5 and 1.0 m in Fig. 11. The trends in most-probable voltage exhibit some intriguing qualities,

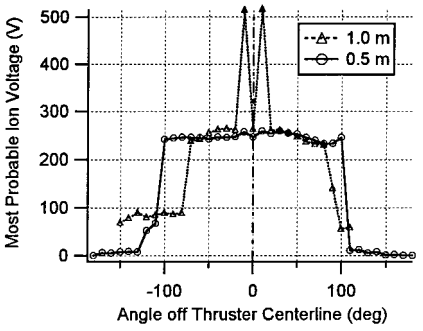

Fig. 11 Most-probable ion voltage (energy/*qe*) as a function of angular position in the plume of the SPT-100 at 0.5- and 1.0-m radius from thruster exit. Uncertainty in V_m < 5 V.

the most striking of which is the existence of high-energy ions at angles exceeding 90 deg from the thrust axis: ions with V_m on the order of 250 V persist out to 100 deg, while particles with V_m nearly 100 V extend to nearly 130 deg at 0.5 m. Although the 1.0-m data show high energy ions up to 100 V at angles of 100 deg, the extent of the 250 V ions is narrower at 1.0 m than at 0.5 m, with these high-energy ions decreasing at 70–80 deg off axis. In general, the trend in angular evolution of most probable ion energy at 1.0 m appears to be a pinched version of that at 0.5 m. This pinching effect may be caused by the configuration of the plasma electric field within the plume. A brief discussion of this effect can be found in Ref. 15.

Although the plasma electric field may explain the narrowing of the highly divergent ions between 0.5 and 1.0 m, the existence of such high-energy ions at angles exceeding 90 deg off axis is still puzzling. Ions with acceleration voltages on the order of the discharge voltage of 300 V should be formed near the upstream end of the thruster acceleration layer (near the anode) and, thus, well upstream of the thruster exit plane. For these ions to be emitted at angles near and exceeding 90 deg off axis, they would have to undergo a considerable curvature in their trajectory upon exiting the thruster because there is no direct line of sight from these points to the inside of the discharge chamber.

Within this picture of the acceleration layer formation, it is apparent that a significant force would be required to deflect high-energy ions originating from deep in the discharge chamber out to trajectories approaching and exceeding 90 deg off axis. The existence of such a force is improbable. It is more plausible that a small amount of propellant ionization and radial acceleration occurs downstream of the discharge chamber exit, external to the thruster. Because the electron mobility is very large along magnetic field lines, within the discharge chamber the magnetic field lines approximate electric equipotentials. Thus ions are formed and accelerated into trajectories normal to the magnetic field line at the ion formation point. Bending of the magnetic field lines (and thus the electric equipotentials) outward from the exit plane would produce a magnetic field fringe with a normal approaching 90 deg. Ions formed within this downstream region would experience an acceleration force perpendicular to the thrust vector and would therefore appear at large angles. Under low enough dynamic pressure inside the vacuum chamber, such a distribution of electric equipotentials may be plausible (private communication by V. Kim, 24 September 1998). It is clearly apparent that this phenomenon is poorly understood and requires further investigation.

C. Multiple Peak Structure

Possibly the most striking feature uncovered in the analysis of the ion-energy distribution function as approximated by $I(V)$ curves was the existence of multiple current peaks suggesting discrete distributions for many angular positions. As can be seen from Fig. 8, these peaks always occurred at discrete multiples of voltage, e.g., a primary peak at $V_b = 260$ V, with secondary peaks at $3V_b/2$, $2V_b$, and $3V_b$. The explanation for this structure is based on the hypothesis of charge-exchange collisions occurring between multiply charged exhaust products and neutral background gas. A detailed discussion of this phenomenon can be found in Refs. 15 and 18; a brief description of the overall mechanism is outlined next.

Consider a charge-exchange collision between an ion with charge $q = 2$ accelerated through a voltage of V_b (having energy $E = qV_b$) and a slow neutral atom. The definition of a charge-exchange collision is an interaction during which one or more electrons are transferred with no significant transfer of kinetic energy between the reactants. Therefore the transfer of an electron from the neutral to the $q = 2$ reactant will produce a slow product ion with charge $q = 1$ along with an ion with kinetic energy still equal to E, but with charge reduced from $q = 2$ to 1. Thus the fast product ion will have an equivalent voltage (energy per charge) of $2V_b$. Such charge-exchange reactions between ions with $q = 2$, 3, and 4 have the capability of producing products with voltages of $\frac{3}{2}$, $\frac{4}{3}$, 2, and 3 times the initial reactant acceleration voltage, depending upon the number of electrons transferred in the collision. Thus the products of such collisions would produce discrete distributions centered at the multiples of the reactant voltages just mentioned. Moreover, the width of the product distributions will be broadened by the multiple of the collision, e.g., in Fig. 8 the initial distribution of reactants extends from 200 to 300 V with a peak at $V_b = 260$ V, thus the product distribution for the $q = 2$ collision extends from 400 to 600 V (twice the width) with a peak at 520 V. The same observances hold true for the peaks located at $\frac{3}{2}$ and 3 V_b.

Thus, the multiple peak structure present in the ion voltage distributions is indicative of reactions involving plume ions with charge $q > 1$ and parasitic neutral gas within the vacuum facility. The number of such collisions should be expected to increase as a function of the path length that the emitted plume ion travels through the neutral background gas. Consider, for example, the traces taken at 30 deg off axis from Figs. 4 and 6. Under the proposed collision scenario those ions possessing voltages greater than 300 V could not have originated from thruster acceleration and must be products of collision. Therefore, the area under the $I(V)$ vs V curve from 0 to 300 V represents the pristine ions that have not undergone a collision, whereas the area under the curve greater than 300 V represents the products of collision. Through a numeric evaluation of such integrals, it is found that 21% of the total ion population at 0.5 m are collision products, with charge-exchange products accounting for 40% of the ion population at 1.0 m.

The charge-exchange cross sections for multiply charged xenon ions on neutrals could not be located in the literature; however, a rough estimate of the expected effect can be made from available data. Using the method of Rapp and Francis, the charge-exchange cross section for Xe^+ on Xe can be calculated as 4×10^{-19} m^2 (Ref. 19). Using this value along with the tank background pressure of 4 mPa yields a collision probability of 24% over a 0.5-m path length and 43% over 1.0 m. Assuming that the cross section of the multiply charged xenon species is on the same order as that of Xe^+ indicates a rough agreement with the findings of this investigation and supports the existence of facility interaction.

The charge-exchange explanation for the existence of high-voltage product peaks implies interesting consequences for the plasma conditions within the thruster discharge chamber. The collision signatures within the voltage distributions imply that the discharge plasma is of sufficient temperature to produce a measureable quantity of ions with $q = 2$ and 3. As further evidence of the thruster internal plasma temperature, consider Fig. 12 showing the ion voltage distribution obtained at −11 deg off axis at 1.0-m radius. In this figure a distribution with a peak at 347 V $= \frac{4}{3}$ V_b is readily apparent. The only possible mechanism to account for such a peak is the reaction between Xe^{4+} and background neutrals, thus the thruster plasma consists of ions with charge states at least up to $q = 4$.

Although charge-exchange collisions can account for the bump-on-tail type of distributions exhibited in this paper, many of the data sets exhibit a long, slowly decaying tail of ions with voltages much greater than that applied to the discharge (300 V). An explanation for this high-voltage tail is detailed in Ref. 15. Briefly, this tail structure is attributed to momentum-transfer collisions occuring between the different charge-state ions within the plume. In such a scenario Xe^{2+} and Xe^+ are accelerated through the same potential, with the Xe^{2+} ion acquiring greater kinetic energy. An elastic collision between theses two ionic species will produce a Xe^+ ion with an effective voltage greater than the applied potential caused by the energy gain

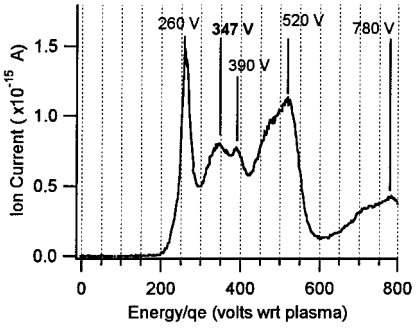

Fig. 12 Ion voltage at 1.0-m radius from the SPT-100 plume at 11 deg off axis showing peaks at $4V_b/3$, $3V_b/2$, $2V_b$, and $3V_b$.

from the Xe^{2+}. Similarly, the Xe^{2+} ion will lose kinetic energy to the collision. The resulting voltage distribution will display tails on both the low-voltage side (caused by Xe^{2+}) and the high-voltage side (caused by Xe^{+}). This type of momentum-transfer collision was found to be more prevalent for regions lying near the thrust vector, with the bump-on-tail signature of the charge-exchange reaction becoming prominent with increasing angle off axis.

VI. Conclusions

One of the most interesting contributions of this research was the measurement of the ion energy at angles exceeding 90 deg off the thrust axis. Although of utmost importance to spacecraft integration, this low-density regime has historically been very difficult to probe. As can be seen by an examination of Fig. 11, V_m is nearly 260 V for all positions within 100 deg of the thrust axis at 0.5 m radius, with $V_m = 90$ V extending all the way around to -150 deg at 1.0-m radius. The mechanism responsible for such high-energy ions extending into the backflow of the plume is not understood. It was previously believed that such high-energy ions must be formed deep within the thruster discharge chamber and would therefore not have a direct line-of-sight path to the plume backflow. Because the existence of the force required to produce a trajectory with sufficient curvature to transport ions formed within the discharge chamber into the backflow is not justified, it is likely that these high-energy ions at large angles were formed downstream of the thruster exit plane and accelerated transverse to the thrust axis at voltages comparable to the applied voltage. These data suggest that the structure of the plasma acceleration region downstream of the thruster exit plane is not accurately explained by current models of Hall-thruster operation.

This research demonstrated direct documentation of facility perturbances on the Hall-thruster plume structure. These parasitic effects were manifested by charge-exchange collisions between plume ions accelerated within the thruster and ambient background neutrals caused by vacuum pumping limitations. As expected, the effect of such collisions increases with ion path length through the imperfect vacuum. Although ion recombination with free plasma electrons in the plume could produce the same distribution shapes as those attributed to charge-exchange collisions, such a recombinative reaction is highly improbable for this plasma.[15]

The facility pressure during testing was approximately 4 mPa, representing a collision probability of 43% at 1.0 m from the thruster for the charge exchange collision between Xe^{+} and background Xe. If a facility with an order-of-magnitude improvement in pressure were used, the collision probability at 1.0 m decreases to 6%. It is apparent, then, that detailed plume characterization in the far field of Hall thrusters (approaching and exceeding 1.0 m) requiring high accuracy should be performed at pressures on the order of 0.4 mPa to reduce parasitic signatures and more correctly quantify effects attributed to the thruster. Some Hall-thruster plume characterization will be insignificantly affected by these facility perturbations. For instance, measurements of plume sputtering on sample materials are fairly insensitive to charge-exchange collisions. Because the sputtering yield is largely dependent only on the incident atom energy (and not on the charge state), the charge-changing character of charge-exchange collisions will not affect the incident atom energy, and the resultant sputtering rate will be unaffected.

Acknowledgments

This research benefited from the generous support of the Air Force Office of Scientific Research represented by Mitat Birkan, the NASA Lewis Research Center with equipment grants administered by John Sankovic, and support from the NASA Johnson Space Center under the direction of Richard Barton. The unique opportunity to evaluate a state-of-the-art thruster was made available by a generous equipment loan from Mike Day of the Space Systems/Loral Company. This support is gratefully acknowledged. Additionally, the authors would like to thank technicians Warren Eaton, Terry Larrow, Gary Gould, Tom Griffin, and Dave McLean for assitance with hardware fabrication. The first author would also like to thank the research staff of Plasmadynamics and Electric Propulsion Laboratory, namely, Matt Domonkos, Colleen Marrese, Frank Gulczinski, James Haas, Sang-wook Kim, and George Williams for their discussions in the preparation of this manuscript.

References

[1] Absalamov, S., Andreev, V., Colbert, T., Day, M., Egorov, V., Gnizdor, R., Kaufman, H., Kim, V., Korakin, A., Kozubsky, K., Kudravzev, S., Lebedev, U., Popov, G., and Zhurin, V., "Measurement of Plasma Parameters in the Stationary Plasma Thruster (SPT-100) Plume and Its Effect on Spacecraft Components," AIAA Paper 92-3156, July 1992.

[2] Myers, R., and Manzella, D., "Stationary Plasma Thruster Plume Characteristics," International Electric Propulsion Conf., IEPC-93-096, Sept. 1993.

[3] Manzella, D., and Sankovic, J., "Hall Thruster Ion Beam Characterization," AIAA Paper 95-2927, July 1995.

[4] Pencil, E., "Preliminary Far-Field Plume Sputtering of the Stationary Plasma Thruster (SPT-100)," International Electric Propulsion Conf., IEPC-93-098, Sept. 1993.

[5] Pencil, E., Randolph, T., and Manzella, D., "End-of-Life Stationary Plasma Thruster Far-Field Plume Characterization," AIAA Paper 96-2709, July 1996.

[6] King, L. B., and Gallimore, A. D., "Propellant Ionization and Mass Spectral Measurements in the Plume of an SPT-100," AIAA Paper 98-3657, July 1998.

[7] King, L. B., Gallimore, A. D., and Marrese, C. M., "Transport Property Measurements in the Plume of an SPT-100 Hall-effect Thruster," *Journal of Propulsion and Power*, Vol. 14, No. 3, 1998, pp. 327–335.

[8] Kim, S. W., Foster, J. E., and Gallimore, A. D., "Very-Near-Field Plume Study of a 1.35-kW SPT-100," AIAA Paper 96-2972, July 1996.

[9] Ohler, S., Gilchrist, B., and Gallimore, A., "Microwave Plume Measurements of an SPT-100 Using Xenon and a Laboratory Model SPT Using Krypton," AIAA Paper 95-2931, July 1995.

[10] Ohler, S. G., Ruffin, A. B., Gilchrist, B. E., and Gallimore, A. D., "RF Signal Impact Study of an SPT," AIAA Paper 96-2706, July 1996.

[11] Pollard, J. E., "Plume Angular, Energy, and Mass Spectral Measurements with the T5 Ion Engine," AIAA Paper 95-2920, July 1995.

[12] deZeeuw, W., va der Ven, H., de Wit, J., and Donne, J., "An Electrostatic Time-of-Flight Analyzer for Simultaneous Energy and Mass Determination of Neutral Particles," *Review of Scientific Instruments*, Vol. 62, No. 1, 1991, pp. 110–117.

[13] Gaus, A., Htwe, W., Brand, T., and Schulz, M., "Energy Spread and Ion Current Measurements of Several Ion Sources," *Review of Scientific Instruments*, Vol. 65, No. 12, 1994, pp. 3739–3745.

[14] Esaulov, V., Grizzi, O., Guillemot, L., Huels, M., Lacombe, S., and Vu Ngoc Tuan, "An Apparatus for Multiparametric Studies of Ion-Surface Collisions," *Review Scientific Instruments*, Vol. 50, No. 2, 1979, pp. 210–218.

[15] King, L. B., "Transport-Property and Mass Spectral Measurements in the Plasma Exhaust Plume of a Hall-Effect Space Propulsion System, Ph.D. Dissertation, Univ. of Michigan, Dept. of Aerospace Engineering, Ann Arbor, MI, May 1998.

[16] Hutchinson, I., *Principles of Plasma Diagnostics*, Cambridge Univ. Press, Cambridge, England, U.K., 1987, pp. 55–66.

[17] Baranov, V., Nazarenko, Y., Petrosov, V., Vasin, A., and Yashnov, Y., "Energy Model and Mechanisms of Acceleration Layer Formation for Hall Thrusters," AIAA Paper 97-3047, Oct. 1991.

[18] King, L. B., and Gallimore, A. D., "Identifying Charge-Exchange Collision Products Within the Ion-Energy Distribution of Electrostatically Accelerated Plasmas," *Physics of Plasmas*, Vol. 6, No. 7, 1999, pp. 2936–2942.

[19] Rapp, D., and Francis, W., "Charge Exchange Between Gaseous Ions and Atoms," *Journal of Chemical Physics*, Vol. 37, No. 11, 1962, pp. 2631–2645.